Ultraviolet Imaging of the Globular Cluster 47 Tucanae

Robert W. O'Connell[1], Ben Dorman[1,2], Ronak Y. Shah[1], Robert T. Rood[1],

Wayne B. Landsman[3], Ralph C. Bohlin[4], Susan G. Neff[2],

Morton S. Roberts[5], Andrew M. Smith[2], and Theodore P. Stecher[2]

ABSTRACT

We have used the Ultraviolet Imaging Telescope to obtain deep far-UV (1620 Å), $40'$ diameter images of the prototypical metal-rich globular cluster 47 Tucanae. We find a population of about 20 hot ($T_{\text{eff}} > 9000$ K) objects near or above the predicted UV luminosity of the hot horizontal branch (HB) and lying within two half-light radii of the cluster center. We believe these are normal hot HB or post-HB objects rather than interacting binaries or blue stragglers. IUE spectra of two are consistent with post-HB phases. These observations, and recent HST photometry of two other metal-rich clusters, demonstrate that populations with rich, cool HB's can nonetheless produce hot HB and post-HB stars. The cluster center also contains an unusual diffuse far-UV source which is more extended than its V-band light. It is possible that this is associated with an intracluster medium, for which there was earlier infrared and X-ray evidence, and is produced by C IV emission or scattered light from grains.

Subject headings: globular clusters: individual—stars: horizontal-branch— ultraviolet: stars—stars: evolution—X-Rays: ISM

[1] Astronomy Dept, University of Virginia, P.O.Box 3818, Charlottesville, VA 22903-0818. Electronic mail: rwo@virginia.edu; dorman@parfait.gsfc.nasa.gov; rys3p@virginia.edu; rtr@virginia.edu

[2] Laboratory for Astronomy & Solar Physics, Code 681, NASA/GSFC, Greenbelt MD 20771. Electronic mail: neff@uit.gsfc.nasa.gov; asmith@uit.gsfc.nasa.gov; stecher@uit.gsfc.nasa.gov

[3] Hughes STX Corporation, Code 681, NASA/GSFC, Greenbelt MD 20771; Electronic mail: landsman@uit.gsfc.nasa.gov

[4] Space Telescope Science Institute, 3700 San Martin Drive, Baltimore, MD 21218; Electronic mail: bohlin@stsci.edu

[5] National Radio Astronomy Observatory, Charlottesville, VA 22903; Electronic mail: mroberts@nrao.edu

1. Introduction

In this paper we report the first wide-field, vacuum ultraviolet imaging of the bright globular cluster 47 Tucanae, in which we have detected both a number of UV-bright, hot stars and an unresolved, extended UV source. Our observations were made as part of the Ultraviolet Imaging Telescope (UIT) survey of globular clusters during the *Astro-2* Spacelab mission in March 1995. The primary astrophysical motivation for the survey was to understand the mechanisms which govern the production of hot stars in horizontal branch (HB) and more advanced evolutionary phases in globular clusters and their relationship to the "UV-upturn" phenomenon in elliptical galaxies (Burstein et al. 1988, Greggio & Renzini 1990).

47 Tuc is the prototype of the class of metal-rich globulars. It has $[Fe/H] \sim -0.7$ and one of the most reliable absolute age determinations (~ 13.5 Gyr; Hesser *et al.* 1987). It is regularly used as a template population to compare to other clusters and the upper giant branches of galaxy color-magnitude diagrams. At optical/infrared wavelengths, the integrated spectral energy distributions of clusters like 47 Tuc are intermediate between those of the more metal-poor globulars and elliptical galaxies. However, they exhibit a unique behavior in the far-UV ($\lambda < 2000$Å) because they have the smallest known ratios of far-UV to optical light of any old populations yet studied (van Albada, de Boer, & Dickens 1981; Rich, Minitti, & Liebert 1993; Dorman, O'Connell, & Rood 1995). The metal-rich globulars therefore represent an important extreme which is important to understand in trying to identify the underlying mechanism of the UV-upturn phenomenon in galaxies. More discussion of these issues can be found in our companion paper on UV imaging of the cluster NGC 362 (Dorman et al. 1997) and in Greggio & Renzini (1990) and Dorman et al. (1995).

Metal-rich globulars are well known for having predominantly red horizontal branches. On the optical-band CMD of Hesser et al. (1987), 47 Tuc has an exclusively red HB, with stars concentrated at $B - V \gtrsim 0.5$. The bluest HB star is a lone RR Lyræ star with $\langle B - V \rangle = 0.40$ ($T_{\rm eff} \sim 6200$ K) (Carney, Storm & Williams 1993). Recent optical-band photometry by Montgomery & Janes (1994, hereafter MJ94) includes several blue HB candidates in the outer parts of the cluster. The only previously-known luminous hot star in 47 Tuc is the very bright ($V = 10.73$, spectral type

B8 III) post-asymptotic giant branch (PAGB) star labeled "BS" by Lloyd Evans (1974).

Earlier vacuum-UV studies of 47 Tuc were made by OAO (Welch & Code 1980), ANS (van Albada et al. 1981), IUE (Rich et al. 1993), and HST/FOC (e.g. Paresce et al. 1991; De Marchi, Paresce, & Ferraro 1993; Paresce, De Marchi, & Jedrzejewski 1995). Except for the early OAO and ANS photometry all these observations were confined to the inner 20″ of the cluster's core (excluding the BS star). HST/FOC identified a number of blue stragglers (BSS) with $T_{\rm eff} < 9000$ K, white dwarfs, and several faint interacting binaries, but no new hot sources near or above HB luminosity. The IUE spectra revealed what appeared to be a warm but spatially extended component which was too faint to consist of objects as bright as the HB.

2. Observations and Data Reduction

A description of the UIT instrument and standard data reduction and calibration procedures is given in Stecher et al. (1997) and Dorman et al. (1997). The field of view is 40′ diameter. Observations were made with a CsI photocathode, which has excellent long-wavelength ("red leak") rejection. We used the B5 filter, which has a peak wavelength of 1620 Å and a bandwidth of 230 Å. In this paper, we use mainly the longest of several 47 Tuc exposures (frame FUV2708, exposure 1680.5 sec), which was also the deepest recorded of any cluster. The images have been digitized to a scale of 1″14/pixel. Point sources have FWHM $\sim 4''$ owing to jitter in the pointing system aboard the Shuttle. Astrometry was obtained using a combination of the Tucholke (1992) and Montgomery & Janes (1994) data for objects in common with the HST Guide Star Catalog. We used an Interactive Data Language (IDL) implementation of DAOPHOT I (Stetson 1987), which has been modified to accommodate the noise characteristics of film, to derive stellar photometry. Typical errors for the photometry are 0.15 mag, including an uncertainty in the aperture correction of 0.10 mag owing to a variable PSF. No correction is necessary for red leaks. We quote FUV magnitudes on the monochromatic system, where $m_\lambda(\lambda) = -2.5 \log(F_\lambda) - 21.1$, and F_λ is in units of erg s^{-1} cm^{-2} Å^{-1}. We refer to B5 magnitudes below as $m(162)$ and $B5 - V$ colors as $(162 - V)$. Due to the failure of UIT's mid-UV camera on the *Astro-2* mission, however, we were unable to

obtain UV colors for our targets. Kent Montgomery (Ph.D. thesis, 1994, Boston University) & Kenneth Janes have kindly provided us with pre-publication CCD BVI photometry of 47 Tuc, a summary of which is given in MJ94.

As basic parameters for 47 Tuc, we adopt the following (Shawl & White 1986; Trager, King & Djorgovski 1995; Djorgovski 1993): $(m - M)_0 = 13.3$; $E(B - V) = 0.04$; $(m - M)_{\mathrm{FUV}} = 13.62$; $r_{0.5} = 174''$ is the half-light radius in the optical band; and integrated $M_V = -9.4$. The optical-band photocenter (J2000) is at $\alpha = 00^{\mathrm{h}} 24^{\mathrm{m}} 05^{\mathrm{s}}.2$, $\delta = -72° 04' 51''$. In computing the FUV apparent distance modulus, we have adopted the Galactic UV reddening law of Cardelli, Clayton & Mathis (1989) according to which $\mathrm{A(FUV)/E(B - V)} = 8.06$.

3. Hot Stars in 47 Tuc

The center of our far-UV image of 47 Tuc is shown in Figure 1 (Plate XX). The brightest object in the field is the previously-known PAGB star, about $45''$ SW of the cluster center. We detect a number of fainter UV point sources, concentrated within the cluster's half-light radius (see inset). Because of the complete suppression of the cool main sequence and red giant branch stars by the UIT detector system, we are able to resolve the hot sources in the cluster throughout the core, which would not be possible at visible wavelengths with our FWHM. Surrounding the cluster center (marked) is a diffuse UV source; this is not a common feature among the clusters we have imaged with UIT, and we return to it in §4.

47 Tuc lies near the Small Magellanic Cloud in projection, and some of the UV-bright stars lying beyond several half-light radii may be SMC main sequence stars. Our large field of view provides a good upper limit to the surface density of such contaminants.

We identified a total of 51 stars in the field with $m(162)$ magnitudes between 9 and 17. At optical wavelengths with ground-based resolution, the cluster center is too dense to make cross-identifications with our UV detections. However, at larger radii ($r \gtrsim 110''$), we have made seven identifications with blue stars ($B - V < 0.2$) in other data sets, as listed in Table 1. Three of these (MJ 280, 33410, 38529) are high probability members of 47 Tuc from proper motions (Tucholke 1992); another (Tucholke # 2497) is a possible member. Four other objects have MJ94 identifications (MJ 8279, 19945, 25308, 38298). The

$(162 - V)$ colors of all these objects are < -1.0, implying $T_{\mathrm{eff}} > 10000\,\mathrm{K}$, and most are < -2. MJ 38298, with $V = 18.75$ has $(162 - V) = -4$, indicating $T_{\mathrm{eff}} \gtrsim 30000\,\mathrm{K}$. Except for MJ 25308 the stars do not have colors and brightnesses consistent with the SMC main sequence. A final identification is with the field star HD 2041 at $10'.35$ radius; this is an F6 IV/V star with $(162 - V) \sim +5.8$.

Positions and photometry for the UIT identifications are given in Table 1. Stars in the table are listed in order of distance from the cluster center. The first column gives the UIT identification number; R is the distance in arcseconds from the cluster photocenter; ΔX is the east-west offset in arcseconds from the cluster center (west being positive); ΔY is the north-south offset in arcseconds from the cluster center (north being positive); $m(162)$ is the monochromatic UV magnitude in the B5 filter (1620 Å centroid); $\sigma(162)$ is the one-sigma uncertainty in the UV magnitude; Q is a subjective estimate of the reality of the sources, ranging from 4 (certain) to 1 (marginal); V and $(B - V)$ are the optical magnitudes and colors from the cross-identifications listed in the Notes column. In the Notes column, MJ = Montgomery & Janes and T = Tucholke.

Since we do not have colors for most sources, our analysis of the resolved population is based mainly on the UV luminosity function, which is shown in Figure 2. In order to assess the SMC contamination, we have plotted the luminosity function in surface density units and for two separate regions of the field: $r < 2\,r_{0.5}$, within which the cluster dominates the counts, and $r > 3\,r_{0.5}$, where SMC stars may be important. 18 of the 51 UV sample stars are within the half-light radius, 22 are within $2\,r_{0.5}$, and 21 are outside $3\,r_{0.5}$. Only 2 of the MJ94 cross-identifications are within $2\,r_{0.5}$. The brightest object is BS, with $m(162) = 9.98\pm0.05$. (BS was observed by Dixon et al. 1995 with the Hopkins Ultraviolet Telescope spectrometer during the *Astro-2* mission, yielding $T_{\mathrm{eff}} \sim 10,500$ K and $\log g < 2.5$.)

TABLE 1
FAR-UV PHOTOMETRY FOR 47 TUCANÆ

UIT ID	R (″)	ΔX	ΔY	$m(162)$	$\sigma(162)$	Q	V	$(B-V)$	Notes
1	17.45	-6.92	16.02	15.46	0.13	4	$\cdots$	$\cdots$	$\cdots$
2	22.23	18.72	-11.99	15.58	0.11	3	$\cdots$	$\cdots$	$\cdots$
3	22.47	-0.74	-22.46	14.85	0.11	4	$\cdots$	$\cdots$	$\cdots$
4	38.12	33.36	18.45	16.24	0.12	2	$\cdots$	$\cdots$	$\cdots$
5	45.63	43.22	14.63	17.45	0.18	2	$\cdots$	$\cdots$	$\cdots$
6	50.12	-11.14	-48.86	15.60	0.12	4	$\cdots$	$\cdots$	$\cdots$
7	51.04	33.16	-38.80	10.30	0.11	4	10.73	$\cdots$	BS, B8III Post-AGB
8	72.33	-72.33	0.76	16.25	0.12	3	$\cdots$	$\cdots$	$\cdots$
9	80.90	-26.53	76.43	17.02	0.13	2	$\cdots$	$\cdots$	$\cdots$
10	89.15	-45.24	76.82	16.74	0.13	2	$\cdots$	$\cdots$	$\cdots$
11	90.36	-71.27	55.54	17.04	0.15	2	$\cdots$	$\cdots$	$\cdots$
12	94.32	13.89	93.29	16.26	0.13	2	$\cdots$	$\cdots$	$\cdots$
13	98.13	24.23	95.09	16.14	0.13	2	$\cdots$	$\cdots$	$\cdots$
14	104.77	89.81	-53.95	13.62	0.10	4	$\cdots$	$\cdots$	IUE spectrum
15	111.66	97.00	-55.31	13.35	0.10	4	15.56	-0.09	MJ19945; IUE spectrum
16	131.02	-35.70	126.07	16.99	0.14	2	$\cdots$	$\cdots$	$\cdots$
17	149.33	-141.58	47.49	14.12	0.11	4	$\cdots$	$\cdots$	$\cdots$
18	151.28	-22.38	149.61	16.15	0.11	3	$\cdots$	$\cdots$	$\cdots$
19	178.54	-101.29	147.03	15.15	0.11	4	$\cdots$	$\cdots$	$\cdots$
20	201.63	157.03	126.48	13.56	0.10	4	$\cdots$	$\cdots$	$\cdots$
21	243.60	-239.86	-42.53	16.25	0.11	3	$\cdots$	$\cdots$	$\cdots$
22	336.08	-182.41	-282.26	13.70	0.10	4	14.43	-0.09	MJ33410, T1948
23	397.84	12.43	-397.64	16.57	0.12	4	$\cdots$	$\cdots$	$\cdots$
24	411.72	-392.66	-123.81	15.07	0.11	4	18.75	$\cdots$	MJ38298
25	415.33	127.51	-395.27	15.71	0.11	4	$\cdots$	$\cdots$	$\cdots$
26	418.80	5.97	418.75	13.60	0.10	4	$\cdots$	$\cdots$	$\cdots$
27	423.91	-422.17	38.37	14.38	0.11	4	$\cdots$	$\cdots$	$\cdots$
28	432.59	409.20	-140.31	15.56	0.11	4	$\cdots$	$\cdots$	$\cdots$
29	492.10	-182.96	456.82	15.51	0.11	4	$\cdots$	$\cdots$	$\cdots$
30	518.75	314.21	412.76	15.86	0.11	4	18.64	-0.17	MJ8279
31	539.12	-406.38	-354.27	13.82	0.11	4	$\cdots$	$\cdots$	$\cdots$
32	558.12	-532.38	-167.52	16.10	0.12	4	$\cdots$	$\cdots$	$\cdots$
33	596.94	-161.79	-574.60	15.79	0.23	1	$\cdots$	$\cdots$	$\cdots$
34	600.95	-598.84	50.26	15.06	0.11	3	$\cdots$	$\cdots$	$\cdots$
35	620.06	612.76	94.89	15.99	0.11	4	$\cdots$	$\cdots$	$\cdots$
36	621.88	-476.36	399.78	13.21	0.10	4	15.01	-0.07	T2497
37	622.52	16.40	-622.31	14.99	0.11	4	$\cdots$	$\cdots$	$\cdots$
38	641.20	215.96	-603.74	16.23	0.31	1	$\cdots$	$\cdots$	$\cdots$
39	653.82	426.76	-495.34	16.21	0.21	1	$\cdots$	$\cdots$	$\cdots$
40	673.56	-480.69	471.83	15.70	0.11	4	$\cdots$	$\cdots$	$\cdots$
41	681.51	681.49	5.08	15.93	0.22	2	$\cdots$	$\cdots$	$\cdots$
42	705.00	-315.04	-630.70	16.31	0.26	1	$\cdots$	$\cdots$	$\cdots$
43	789.04	-709.61	-345.01	16.56	0.25	1	$\cdots$	$\cdots$	$\cdots$
44	817.30	-811.76	94.97	15.90	0.11	3	$\cdots$	$\cdots$	$\cdots$
45	821.41	721.75	392.16	13.18	0.11	4	$\cdots$	$\cdots$	$\cdots$

4

TABLE 1—*Continued*

UIT ID	R ($''$)	ΔX	ΔY	$m(162)$	$\sigma(162)$	Q	V	$(B-V)$	Notes
46	864.98	-5.77	-864.96	16.32	0.24	1	15.23	-0.16	MJ280, T300
47	906.97	-854.97	-302.71	15.45	0.21	1	$\cdots$	$\cdots$	$\cdots$
48	943.11	602.48	-725.58	14.28	0.10	4	$\cdots$	$\cdots$	$\cdots$
49	947.46	-628.16	-709.28	15.63	0.11	3	$\cdots$	$\cdots$	$\cdots$
50	960.44	-414.76	866.27	14.32	0.11	3	$\cdots$	$\cdots$	$\cdots$
51	962.44	156.68	-949.60	16.18	0.11	4	$\cdots$	$\cdots$	$\cdots$

The modes of both the inner and outer histograms plotted occur at $m(162) = 15$–16. It is not clear whether the decline at fainter magnitudes is intrinsic or is instead produced by the sensitivity limit of the data. There is a clear excess (a factor of $7\times$ at the mode) in the surface density of detections for the inner field. Most of the detections here are therefore members of 47 Tuc. The astrometric study of Tucholke (1992) found an "almost a complete lack of SMC stars" brighter than a limit of $B \sim 17$, which is consistent with these results.

The brightest objects other than BS lie at $m(162) = 13$–14, which (see below) is above the expected brightness of the HB in 47 Tuc. Two of these supra-HB stars are located within $7''$ of each other, approximately $2'$ southwest of the cluster center. One of these (UIT-15) is identified with MJ 19945 ($V = 15.56$, $B - V = -0.09$) while the other (UIT-14) is unidentified in the optical. On 11-Sep-1995, we obtained a 400 minute low-dispersion IUE image (SWP 55910), with the large ($10 \times 20''$) aperture centered between the two stars. A spectrum for each star was extracted from the line-by-line IUE image, and is presented in Figure 3. The UV spectrum and V magnitude of MJ 19945 are well-fit by a Kurucz (1993) model with $T_{\rm eff} = 14000\,{\rm K}$, $\log g = 3.5$, and $[{\rm Fe/H}] = -0.5$. The best-fit model of UIT-14 has $T_{\rm eff} = 50000\,{\rm K}$ and $\log g = 5.0$, though the fit is not as good, and the IUE spectrum does not provide good discrimination for $T_{\rm eff} > 30000\,{\rm K}$. UIT-14 is almost certainly a member of 47 Tuc, given its very high temperature (characteristic of an sdO star) and proximity to the cluster center. In both cases, the IUE data confirm the UIT flux measurements and the expectation that mainly high temperature objects will be present on the UIT image.

For comparison to the luminosity function in Fig. 2, we have created a synthetic UV-optical CMD for 47 Tuc in observed coordinates (Figure 4). We transformed the model ZAHB and main sequence for $[{\rm Fe/H}] = -0.78$ from D'Cruz et al. (1996) by interpolation in the model atmosphere grid of Kurucz (1993). Extinction effects were incorporated based on the assumptions stated in Sec. 2. We have included in the figure the brightest blue stragglers from the HST/FOC UV photometry of De Marchi et al. (1993) and also from the recent HST/WFPC2 optical-band photometry of Sosin et al. (1997). In both cases, we have transformed optical-band photometry to the UV using the Kurucz atmospheres. This is relatively

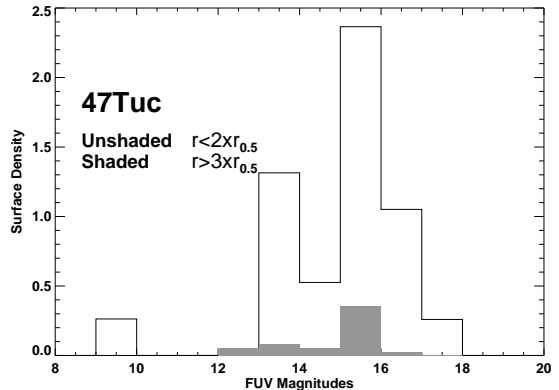Fig. 2.— Histogram of the surface densities of UV identifications for the inner and outer regions of 47 Tuc as a function of UV brightness. Units are 10^{-5} stars per square arcsecond.
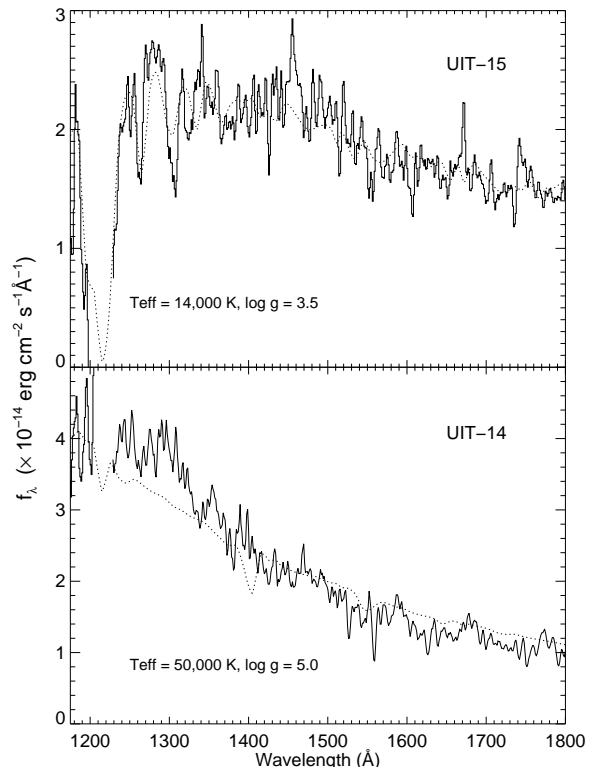

Fig. 3.— IUE low-resolution, far-UV spectra of two of the supra-HB identifications in 47 Tuc. Overplotted are the best fitting model atmospheres, as described in the text. UIT-15, the cooler object, is MJ 19945.

6

crude but suffices to indicate where the known BSS stars should appear in our counts. Note that the field covered by the WFPC2 sample extends to $r \leq 110''$ and includes only 6% of the area of the $2\,r_{0.5}$ UIT sample.

Given our limiting magnitude of $m(162) \sim 17$, we see from Fig. 4 that we should not detect HB stars cooler than $B - V \sim 0.18$ ($T_{\text{eff}} \sim 8300\,\text{K}$) or blue straggler stars cooler than $B - V \sim 0.05$ ($T_{\text{eff}} \sim 10000\,\text{K}$). The known HST blue stragglers should all fall at $m(162) \gtrsim 16.5$. The great majority of the BSS which Paresce et al. (1991) detected in the core of 47 Tuc with a surface density of $\sim 0.05\,\text{arcsec}^{-2}$ are too cool to be detected here, but some of the stars in the two faintest bins of Fig. 2 are probably BSS.

We cannot make an unambiguous identification of the kind of stars in the most populated bin ($m[162] = 15$–16) in our luminosity function (Fig. 2). A well populated extreme HB branch (with $B - V < -0.05$) should appear about one magnitude brighter (see Fig. 4), and the two independent HST studies agree that the BSS objects probably fall at least one magnitude fainter. Based on the calibration in Fig. 4, the modal bin corresponds to HB stars in the range $B - V \sim 0.0$–0.1, $V > 16$. It is not clear how well this region has been explored in existing optical-band CMD's.

It is possible that the mode of the luminosity function in Fig. 2 does correspond to the extreme horizontal branch if the theoretical calibration in Fig. 4 slightly overpredicts the hot HB luminosity. We encountered this circumstance in several other clusters observed with UIT (e.g. NGC 1851, Parise et al. 1994; and ω Cen, Whitney et al. 1994). The number of probable post-HB stars in the luminosity function also favors this interpretation. The models in Fig. 4 predict that extreme HB stars should not be brighter than $m(162) \sim 14$. The five objects in the $m(162) = 13$–14 bin are therefore supra-HB stars, probably in post-HB evolutionary phases moving coolward in the CMD toward the asymptotic giant branch or upward in the CMD as "AGB-Manquè" objects (e.g. Greggio & Renzini 1990; Dorman, Rood, & O'Connell 1993). The presence of a few objects of this type has also been inferred in other metal-rich clusters from IUE spectroscopy (Rich et al. 1993), and the RR Lyrae object in 47 Tuc is probably another example (Carney et al. 1993). The evolutionary lifetimes of these post-HB phases, however, are such that one expects about 4 times as many blue HB precursors. Only by interpreting the mode of the luminosity function in Fig. 2 as representing the blue HB can the density of supra-HB stars be made roughly consistent with canonical evolutionary theory.

An alternative intepretation of the supra-HB stars as interacting binaries (e.g. Rich et al. 1993) is unlikely, given the facts that almost all such objects have luminosities below the HB and that UIT-14 and MJ 19445 seem to have normal spectra for post-HB phases. No emission lines are present in the spectra. A more exotic interpretation of the supra-HB stars is that they are due to binary mergers of helium white dwarfs (Iben 1990, Bailyn 1995), which is a process that can yield core helium-burning stars with core masses of up to $0.8\text{M}_\odot$. This is the preferred explanation for two hot supra-HB stars in M3, which lacks an extended blue HB (Buzzoni et al. 1992). 47 Tuc is known to have many types of exotic stars, including one-third of all known millisecond pulsars (Robinson et al. 1995), which are likely created by binary processes. It is not unreasonable that a small number of binary mergers could be responsible for the supra-HB stars, given the cluster's large total population, but we cannot test that possibility now. Further optical or UV photometry of the hot population will be needed to determine whether a genuine blue HB is present.

We therefore believe that the hot population we have detected within $2\,r_{0.5}$ in 47 Tuc consists (in declining luminosity order) of one PAGB star (BS), 5–6 other stars in post-HB evolution, 9–15 hot HB stars (somewhat fainter than expected from canonical theory), and a few BSS objects at the threshold of our photometry. This separation is, however, not unambiguous, and colors will have to be obtained to make positive classifications. The small subsample with IUE or optical data does tend to confirm this separation.

4. Diffuse Far-UV Emission

An unexpected feature of the UIT image is the presence of a diffuse far-UV component in the cluster center (see Fig. 1). The component is also detectable on a shorter UIT exposure (FUV2388, exposure 1031 sec) taken on a different orbit. This may be the same component first reported by Rich et al. (1993) on IUE spectra of the inner $20''$ of the cluster, and our central surface brightness value agrees with their IUE

continuum value (but see qualifying comments below on the IUE spectra). The diffuse light is symmetrical about the cluster center coordinates and is detectable up to a radius of $500''$. There is a low-level, asymmetric background, probably skyglow, on the deeper UIT images which prevents us from making accurate measures at larger radii; within $400''$, however, the photometry is reliable. The adopted background level is the mean flux in an annulus centered on the cluster with inner and outer radii of 600 and $700''$. Tests show that instrumental scattered light from the bright PAGB star has negligible influence on the cluster surface brightness at distances larger than $25''$ from the star. The integrated brightness of the diffuse component is relatively large. After all resolved stars are masked out of the image, the diffuse light has $m(162) = 10.2 \pm 0.2$ within $r_{0.5}$, corresponding to 40% of the total FUV light in that region, and $m(162) = 9.4 \pm 0.3$ within $400''$ (58%).

The surface brightness profile of the diffuse component is shown in Figure 5. We have compared this distribution to that of the cluster's integrated V-band light from Trager et al. (1995) and computed the $(162-V)$ color profile also shown in Fig. 5. There is a large color gradient, from $(162-V)$ values of ~ 6 mags at the center to significantly bluer values ~ 4 mags by $300''$ radius. This means that the diffuse FUV light is significantly *less* concentrated than the bulk of the stellar population. Since the UV background level is somewhat uncertain, we have checked that adopting different background levels within a plausible range does not affect the color gradient within a radius of $200''$.

Among clusters observed by UIT, only M79 has a similar diffuse feature (Hill et al. 1996). Most clusters on the UIT program have too many UV-bright stars to detect a diffuse component easily. The central regions of M79 are unresolved by UIT; beyond $1'$ from the core a diffuse component is detectable at a surface brightness $\lesssim 1$ mag fainter than the total light. Unlike the source in 47 Tuc, the diffuse UV light of M79 appears to parallel the V-band light distribution.

The simplest explanation for the diffuse UV component in 47 Tuc would be that it is the combined light of the warm stars which are just below the threshold for detection as individual objects in Fig. 4. However, in the case of normal warm HB stars, one would expect the FUV light to follow the distribution of V-band light; and in the case of BSS stars, it should be much more concentrated to the cluster
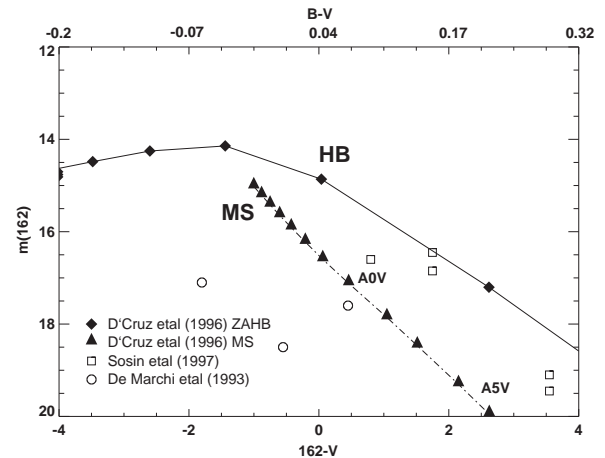

Fig. 4.— A synthetic UV-optical color-magnitude diagram for 47 Tuc, in which the theoretical locations of the ZAHB and the main sequence have been transformed to observational quantities after adopting standard parameters for the cluster given in the text. Approximate locations of the brighter blue stragglers detected in HST observations of the cluster core are plotted individually.
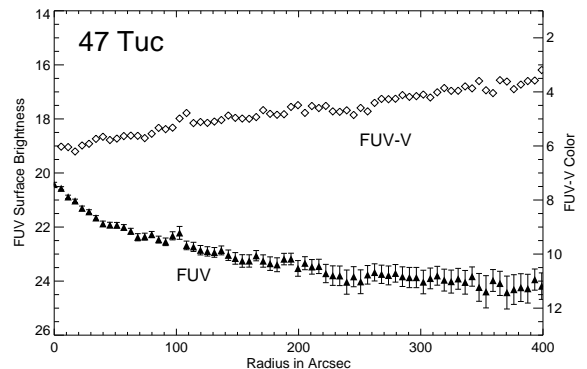

Fig. 5.— Surface photometry of the diffuse far-UV component in 47 Tuc. All stars have been masked out. The solid triangles show the mean surface brightness in circular annuli; units (left hand scale) are monochromatic UV magnitudes per square arcsecond. The open diamonds are the FUV–V colors (right hand scale) obtained by subtracting the Trager et al. (1995) V-band surface brightnesses at the same locations. Details on the background correction are given in the text.

center than the V-band light (Paresce et al. 1991). In contrast, the diffuse FUV component is more extended than the V-band light. Some binary models for hot cluster stars produce such distributions (e.g. Bailyn et al. 1992; Bailyn 1995), but it seems unlikely that there would be enough such objects just below the UIT threshold to produce the observed diffuse source.

Another possibility is that the diffuse far-UV light is not stellar. Krockenberger & Grindlay (1995) have recently discovered a bow-shock-like feature associated with 47 Tuc using ROSAT in the 0.1–0.4 keV X-ray band. We do not detect any far-UV enhancement near the X-ray feature (about $6.'5$ NE of the cluster center), but the presence of a possible bow shock suggests that 47 Tuc contains a significant component of interstellar gas. Presumably, this is the remains of the stellar envelopes which have been shed during RGB mass loss. The most likely far-UV signature of this material would be the C IV 1550 Å emission feature. Assigning all of the diffuse emission to C IV, we have estimated the gas temperature and density necessary to produce the far-UV surface brightness assuming that the intracluster gas is collisionally ionized and in pressure equilibrium with the shocked material at the interface with the Galactic halo. For the carbon abundance of 47 Tuc, we find that an electron temperature of $\sim 50000\,$K and $n_e \sim 0.05\,\mathrm{cm}^{-3}$ over $r_{0.5}$ would yield the observed surface brightness. The total amount of material needed ($\sim 0.3\mathrm{M}_\odot$) corresponds to the accumulation of mass lost from the RGB (assuming $0.2\mathrm{M}_\odot$ lost per giant) over a period of $\sim 3 \times 10^5$ years, roughly consistent with the residence time for gas in the cluster given its velocity with respect to its surroundings. Therefore, on the basis of its X-ray properties and the estimated RGB mass loss rate, C IV emission from an intracluster medium is a plausible source of the diffuse far-UV light in 47 Tuc.

Unfortunately, C IV emission is not detected on three large aperture ($10\times20''$) spectra of the center of 47 Tuc in the IUE archives. Two of these (SWP 1510 and 2086) were discussed by Rich et al. (1993). They show an extended but nonuniform far-UV continuum at a level of about $5\times10^{-15}\,\mathrm{erg\ s^{-1}\ cm^{-2}\ \mathring{A}^{-1}}$, which is consistent with the mean far-UV surface brightness determined by UIT for the cluster center ($2.3 \times 10^{-17}\,\mathrm{erg\ s^{-1}\ cm^{-2}\ \mathring{A}^{-1}\ arcsec^{-2}}$) when integrated over the IUE aperture. No emission lines are visible. These spectra are from early in the IUE mission before operations procedures had been standard-ized; they are noisy, and SWP 1510 is out of focus. A later spectrum, SWP 11126, with an exposure time of 49.5 kilosec, shows no detectable far-UV flux at all, with an upper limit of $3 \times 10^{-15}\,\mathrm{erg\ s^{-1}\ cm^{-2}\ \mathring{A}^{-1}}$. These results are contradictory. Ordinarily, one would give more weight to the more recent spectrum, but it is possible that the difficulty in centering IUE on a diffuse object led to a pointing error in that case. An offset of order $20''$ would reduce the mean diffuse flux a factor of two. Even in that case, however, if the far-UV flux detected by UIT were concentrated in the C IV emission doublet, the resulting feature would have been easily detected. Because of the inconsistencies in the IUE data, it is premature to rule out the C IV interpretation, but the available spectra do not support it.

A final possibility is that the diffuse UV light is produced by scattering of stellar UV photons by dust grains. Gillett et al. (1988) detected a small excess over photospheric emission at 100μ in 47 Tuc with IRAS, which they attributed to intracluster dust grains heated by the cluster's integrated starlight. They estimated the total dust mass at $3 \times 10^{-4}\mathrm{M}_\odot$. But they pointed out that this is 100–1000 times smaller than expected given the standard RGB injection rate and a residence time of 3×10^7 yrs based on the interval between Galactic plane crossings. However, if the residence time is reduced to only a few 10^5 years by virtue of the cluster-halo interaction demonstrated by Krockenberger & Grindlay (1995), then the dust mass is in much better agreement with predictions. In the UV, dust grains are strongly forward scattering (Witt et al. 1992), and any UV-bright source on the far side of the cluster center might well produce a detectable diffuse UV component. The obvious candidate is the very bright PAGB star BS. Whether the brightness and symmetry of the diffuse light is consistent with scattering cannot be decided without quantitative modeling. One might expect the grains produced in a sub-solar abundance system like 47 Tuc to more resemble those in the SMC than those typical of our Galaxy (e.g. Hutchings 1982, Mathis 1990).

5. Summary and Discussion

5.1. Hot Stars

UIT images at 1500 Å of a $40'$ diameter field centered on the metal rich globular cluster 47 Tuc have disclosed a population of 51 hot stars, many of which

are probably cluster members. We do not have colors for most of these objects, so our analysis is based on their UV luminosity function. About 20 of the sample lie near or above the predicted UV luminosity of the hot horizontal branch (HB) and are within two half-light radii of the cluster center. IUE spectra of two of these are consistent with post-HB phases. Overall, the sample within $2\,r_{0.5}$ in 47 Tuc probably consists (in declining luminosity order) of one PAGB star (BS), 5–6 other stars in post-HB evolution, 9–15 hot HB stars (somewhat fainter than expected from canonical theory), and a few BSS objects at the threshold of our photometry. This separation requires confirmation by multicolor photometry. We cannot rule out the possibility that the supra-HB stars are merged binaries rather than normal post-HB objects.

The UV-bright population of 47 Tuc demonstrates that populations with metallicities as high as those of metal-rich globular clusters and with dominant cool horizontal branches can nonetheless produce hot HB stars. Extreme HB stars and their subsequent hot He-shell-burning evolutionary phases are the likely source of the "UV-upturns" seen in elliptical galaxies (Greggio & Renzini 1990; Dorman et al. 1995; Brown, Ferguson, & Davidsen 1996). This type of object evidently exists in 47 Tuc, even if the numbers are too small to produce a net upturn in its far-UV energy distribution.

Over the past 10 years, deep optical and UV observations have shown that many low metallicity globular clusters have bimodal or extended horizontal branch mass distributions which include objects at high temperature. Examples include NGC 2808 (Ferraro et al. 1990; Sosin et al. 1997), NGC 1851 (Walker 1992), M15 (Crocker, Rood, & O'Connell 1988), ω Cen (Whitney et al. 1994), M79 (Hill et al. 1996), NGC 6752 (Landsman et al. 1996), and NGC 362 (Dorman et al. 1997). Our UV observations of 47 Tuc and recent optical-band HST imaging of the centers of two other metal rich clusters NGC 6388 and NGC 6441 (Piotto et al. 1997, Rich et al. 1997) show that this phenomenon extends to clusters of high metallicity. Indeed, the observations of NGC 6388 and NGC 6441 (which were not included in the UIT program because of heavy UV foreground extinction) show that the fraction of hot HB stars in metal rich clusters can be significant.

For the purposes of understanding the galaxies, it is important to understand how such hot objects are produced in clusters, particularly metal-rich clusters.

Is red giant branch mass loss in single stars alone responsible, or are multi-object processes, such as binary mass exchange, binary mergers, or dynamical interactions with neighbors important (Iben 1990, Fusi-Pecci et al. 1993, Bailyn 1995)? Do several modes operate within a given cluster? There is some evidence that dynamical interactions promote hot HB's in some instances (Fusi-Pecci et al. 1993). On the other hand, the largest population of EHB and post-EHB stars yet found resides in the low density cluster ω Cen (Whitney et al. 1994). Rich et al. (1997) tend to favor the dynamical explanation for the HB's of NGC 6388 and 6441, despite the absence of the expected strong radial gradients in the blue population. 47 Tuc is nearly as dense as these two objects and contains hot stars, yet its hot population is much smaller. Also, the surface density of the UIT sample of hot stars in 47 Tuc, when normalized to the Trager et al. (1995) V-band surface brightness, increases by at least a factor of two from the region inside $r_{0.5}$ to regions at 1–3 $r_{0.5}$. This is again contrary to expectations for most multi-object processes.

Whatever the clusters may be telling us about the possible dynamical origin of hot HB stars, the dynamical environment of elliptical galaxies is very different from clusters. Striking variations in UV properties are observed among the galaxies, in the form of differences in the central UV colors (Burstein et al. 1988) and in strong gradients in UV colors (O'Connell et al. 1992, Ohl et al. 1997). It seems unlikely that multi-object processes in the general gravitational field of the galaxies are important to producing these effects. If the UV-bright stars in the galaxies were never members of dense stellar aggregates, then the clusters most relevant to the galaxies are those without strong dynamical effects on their hot star populations. On the other hand, if the hot stars originated in globular clusters which were later destroyed by tidal interactions, then the dynamical properties of the parent clusters could play a role if a large proportion of close binaries were generated. In any event, until the origin of HB mass distributions is better understood, through the study of the clusters, it is premature to try to derive global properties such as age or abundance from the UV-upturns of galaxies.

5.2. Diffuse Light

The UIT images also reveal a diffuse source in 47 Tuc which can be traced to radii $\gtrsim 500''$. The UV light is more extended than the V-band light, which

produces a strong UV–V color gradient, with bluer colors at larger radii. There is no good stellar candidate for the source of this light. We consider possible non-stellar radiation from an intracluster medium which, from ROSAT and IRAS observations, does seem to be present in 47 Tuc. Line emission from C IV is plausible based on expected physical conditions in the intracluster medium. The line is not confirmed by IUE spectra, but these have inconsistent characteristics. Scattering by dust grains of light from the bright PAGB star is another possibility.

REFERENCES

Bailyn, C. D. 1995, ARAA, 33, 133

Bailyn, C. D., Sarajedini, A., Cohn, H., Lugger, P. M., & Grindlay, J. E. 1992, AJ, 103, 1564

Brown, T. H., Ferguson, H. C., & Davidsen, A. F. 1995, ApJ, 454, L15

Burstein, D., Bertola, F., Buson, L. M., Faber, S. M., & Lauer, T. R. 1988, ApJ, 328, 440

Buzzoni, A., Cacciari, C., Fusi Pecci, F., Buonanno, R. & Corsi, C. E. 1992, A&A, 254, 110

Cardelli, J., Clayton, G. C., & Mathis, J. S. 1989, ApJ, 345, 245

Carney, B., Storm, J., & Williams, C. 1993, PASP, 105, 294

Crocker, D. A., Rood, R. T., & O'Connell, R. W. 1988, ApJ, 332, 236

D'Cruz, N., Dorman, B., Rood, R. T., & O'Connell, R. W. 1996, ApJ, 466, 359

De Marchi, G., Paresce, F., & Ferraro, F. 1993, ApJS, 85, 293

Dixon, W. V., *et al.* 1995, ApJ, 454, L47

Djorgovski, S. G. 1993 in The Structure and Dynamics of Globular Clusters ed. S. G. Djorgovski & G. Meylan (ASP: San Francisco), p.373

Dorman, B., Rood, R.T., & O'Connell, R. W. 1993, ApJ, 419, 596

Dorman, B., O'Connell, R. W., & Rood, R. T., 1995, ApJ, 442, 105.

Dorman, B., et al. 1997, ApJ, in press

Ferraro, F. R., Clementini, G., Fusi Pecci, F., Buonanno, R., & Alcaino, G. 1990, A&AS, 84, 59

Fusi Pecci, F., Ferraro, F. R., Bellazzini, M., Djorgovski, D. S., Piotto, G., & Buonanno, R. 1993, AJ, 105, 1145

Gillett, F. C., de Jong, T., Neugebauer, G., Rice, W. L., & Emerson, J. P. 1988, AJ, 96, 116

Greggio, L. & Renzini, A. 1990 ApJ, 364, 35

Hesser, J. E., Hartwick, F. D. A., VandenBerg, D. A., Allwright, J. W. B., Shott, P., & Stetson, P. B., 1987, PASP, 99, 739

Hill, R. S., et al. 1996, AJ, 112, 601

Hutchings, J. B. 1982, ApJ, 255, 70

Iben, I. 1990, ApJ, 353, 215

Kurucz, R.L. 1993, "ATLAS9 Stellar Atmosphere Programs and 2 km/s grid", CD-ROM No. 13, Smithsonian Astrophysical Observatory

Krockenberger, M. & Grindlay, J. E. 1995, ApJ 451, 200

Landsman, W. B. et al. 1996, ApJ 472, L93

Lloyd Evans, T. 1974, MNRAS, 167, 393

Mathis, J. S. 1990, ARAA, 28, 37

Montgomery, K. A. & Janes, K. A. 1994 in Hot Stars in the Halo eds. S. J. Adelman, A. R. Upgren, & C. J. Adelman, pp. 136–148. [MJ94]

O'Connell, R. W. et al. 1992, ApJ, 395, L45

Ohl, R. G. et al. 1997, in preparation

Paresce, F. et al. 1991, Nature, 352, 297

Paresce, F., De Marchi, G., & Jedrzejewski, R. 1995, ApJ, 442, L57

Parise, R. A. et al. 1994, ApJ, 423, 305

Piotto, G. et al. 1997, in Advances in Stellar Evolution, eds. R. T. Rood & A. Renzini (Cambridge: Cambridge Univ. Press), in press

Rich, R. M., Minniti, D., & Liebert, J. W. 1993, ApJ, 406, 489

Rich et al. 1997, ApJ, in press

Robinson, C., Lyne, A. G. Manchester, R. N., Bailes, M., D'Amico, N. 1995, MNRAS, 274, 147

Shawl, S. & White R. 1986, AJ, 91, 312

Sosin, C. et al. 1997, in preparation

Stecher, et al. 1997, PASP, in press

Stetson, P. B. 1987, PASP, 99, 191

Trager, S. C., King, I. R., & Djorgovski, S. G. 1995, AJ, 109, 218

Tucholke, H.-J. 1992, A&AS, 93, 293

van Albada, T. S., de Boer, K. S., and Dickens, R. J. 1981, MNRAS, 195, 591

Walker, A. R. 1992, PASP, 104, 1063

Welch, G. A. & Code, A. D. 1980, ApJ, 236, 798

Whitney, J. et al. 1994, AJ, 108, 1350

Witt, A.N., Petersohn, J. K., Bohlin, R. C., O'Connell, R. W., Roberts, M. S., Smith, A. M., & Stecher, T. P. 1992, ApJ, 395, L5

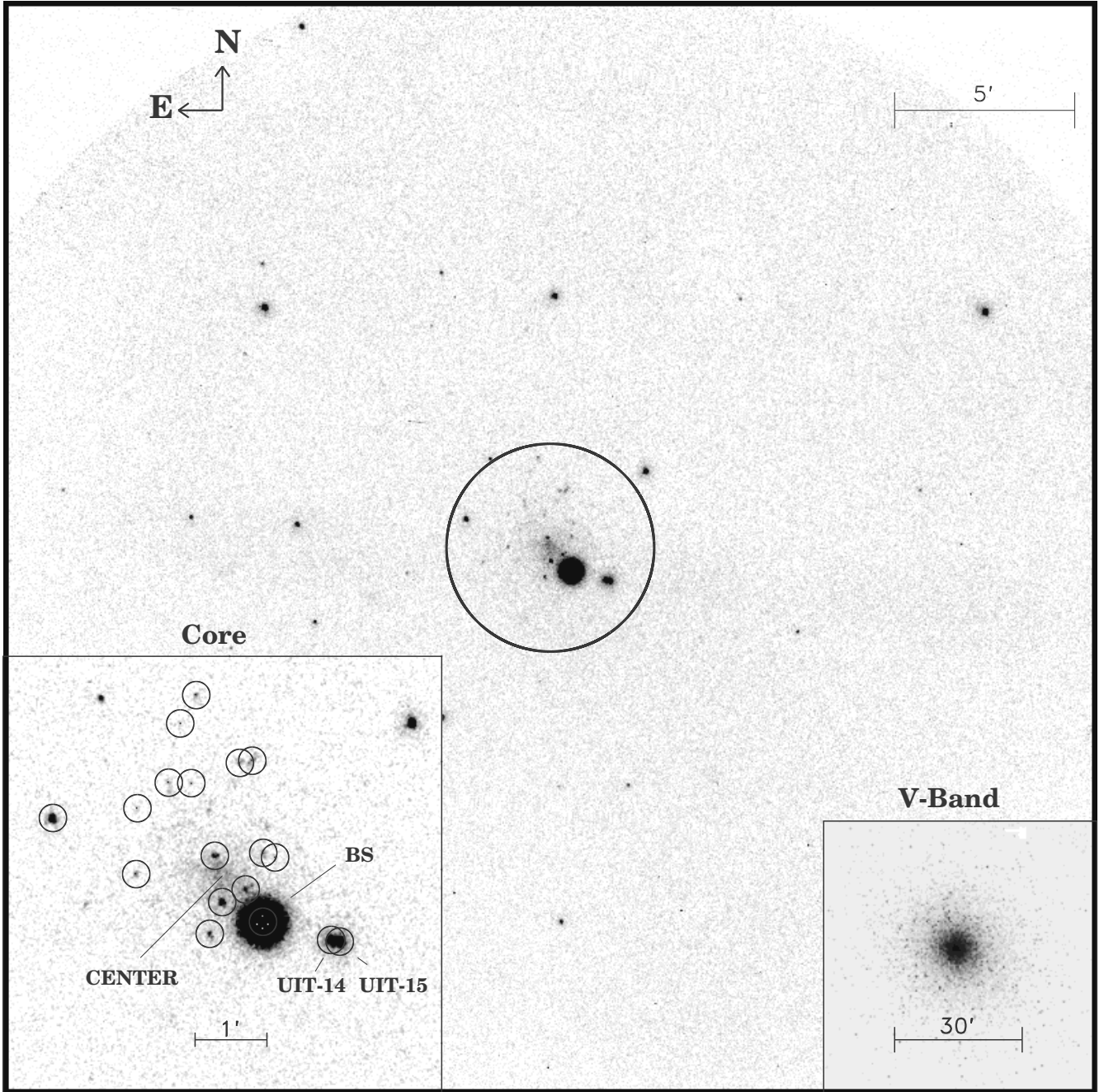Fig. 1.— (Plate XX) The Ultraviolet Imaging Telescope far-ultraviolet (1620 Å) image of 47 Tuc. The full field of view is $40'$ in diameter; the edge of the field is visible at the top. The heavy line in the main image shows the circle containing half the cluster light at optical wavelengths. The inset at the lower right shows the cluster in the V band; the inner few arcminutes are burned out by cool main sequence and giant-branch stars which are suppressed in the UV. The inset at the left is an enlargement of the center of the UV image showing all of the UV identifications within the half-light radius. The diffuse light component discussed in §4 is just visible on the main and UV inset images.